Hindawi
Adsorption Science & Technology
Volume 2023, Article ID 9803690, 1 page
https://doi.org/10.1155/2023/9803690

Retraction

Retracted: Antioxidant, Antimicrobial, and Photocatalytic Potential of Cobalt Fluoride (CoF_2) Nanoparticles

Adsorption Science and Technology

Received 19 December 2023; Accepted 19 December 2023; Published 20 December 2023

This article has been retracted by Hindawi following an investigation undertaken by the publisher [1]. This investigation has uncovered evidence of one or more of the following indicators of systematic manipulation of the publication process:

(1) Discrepancies in scope

(2) Discrepancies in the description of the research reported

(3) Discrepancies between the availability of data and the research described

(4) Inappropriate citations

(5) Incoherent, meaningless and/or irrelevant content included in the article

(6) Manipulated or compromised peer review

The presence of these indicators undermines our confidence in the integrity of the article's content and we cannot, therefore, vouch for its reliability. Please note that this notice is intended solely to alert readers that the content of this article is unreliable. We have not investigated whether authors were aware of or involved in the systematic manipulation of the publication process.

Wiley and Hindawi regrets that the usual quality checks did not identify these issues before publication and have since put additional measures in place to safeguard research integrity.

We wish to credit our own Research Integrity and Research Publishing teams and anonymous and named external researchers and research integrity experts for contributing to this investigation.

The corresponding author, as the representative of all authors, has been given the opportunity to register their agreement or disagreement to this retraction. We have kept a record of any response received.

References

[1] J. Khan, H. Ullah, R. Ullah et al., "Antioxidant, Antimicrobial, and Photocatalytic Potential of Cobalt Fluoride (CoF_2) Nanoparticles," *Adsorption Science & Technology*, vol. 2022, Article ID 9369201, 6 pages, 2022.

Hindawi
Adsorption Science & Technology
Volume 2022, Article ID 9369201, 6 pages
https://doi.org/10.1155/2022/9369201

Research Article

Antioxidant, Antimicrobial, and Photocatalytic Potential of Cobalt Fluoride (CoF_2) Nanoparticles

Jamshid Khan,[1] Hameed Ullah,[2] Riaz Ullah,[3] Muhammad Sajjad,[4] Khalid Hussain Thebo,[5] Amal Alotaibi,[6] Muhammad Zahoor,[7] Nadia Bukhari,[8] and H. C. Ananda Murthy[9]

[1]*Department of Chemistry, Hazara University Mansehra, 21300 Khyber Pakhtunkhwa, Pakistan*
[2]*Department of Chemistry, Islamia College University, Peshawar 25120 -Khyber Pakhtunkhwa, Pakistan*
[3]*Department of Pharmacognosy, College of Pharmacy, King Saud University, Riyadh, Saudi Arabia*
[4]*Department of Physics, Kohat University of Science and Technology, Kohat, 26000 Khyber Pakhtunkhwa, Pakistan*
[5]*Institute of Metal Research, Chinese Academy of Sciences, 72 Wenhua Road, Shenyang 110016, China*
[6]*Department of Basic Science, College of Medicine, Princess Nourah Bint Abdulrahman University, P.O. Box 84428, Riyadh 11671, Saudi Arabia*
[7]*Department of Biochemistry, University of Malakand, Chakdara, Dir Lower, 18800 KPK, Pakistan*
[8]*Department of Chemistry, Kohat University of Science and Technology, Kohat, 26000 Khyber Pakhtunkhwa, Pakistan*
[9]*Department of Applied Chemistry, School of Applied Natural Science, Adama Science and Technology University, P.O. Box 1888, Adama, Ethiopia*

Correspondence should be addressed to H. C. Ananda Murthy; anandkps350@gmail.com

Received 31 January 2022; Accepted 29 March 2022; Published 12 April 2022

Academic Editor: Lakshmipathy R

Herein, CoF_2 nanoparticles (NPs) are prepared by simple coprecipitation method and are characterized by various techniques, i.e., XRD, SEM/EDX, FTIR, and UV/Vis, for their structure identification. As-prepared nanostructures were used as photocatalyst, as antioxidant, and as antimicrobial agent. The degradation studies of the prepared samples were carried out for specific time for the degradation of methylene blue (MLB) dye under a UV/visible spectrophotometer to determine decolorization and change in concentration of MLB with respect to time. The antibacterial activity against *Escherichia coli* (*E. coli*) and *Bacillus subtilis* (*B. subtilis*) was measured by well diffusion and serial dilution method to determine their efficiency against these two bacteria, through a dose-dependent method. The antibacterial activity was further confirmed against the experimental bacteria through calculation of minimum inhibition concentration (MIC). The antioxidant activity (radical scavenging activity) of the prepared CoF_2 NPs was also assessed.

1. Introduction

The utilization of matter at the nanoscale (1-100 nm), i.e., atomic, molecular, or supramolecular, for commercial and industrial applications is related to nanotechnology. Quantum confinement and size are the important aspects of the nanomaterials for the development of devices and commercial products [1, 2]. Nanotechnology includes a variety of fields, and on the basis of size, nanomaterials have diverse applications including energy storage, surface chemistry, semiconductor, catalysis, organic chemistry, engineering, biology, thin layer, and self-assemblies [3–5]. Various types of semiconductor oxide and sulphide like TiO_2, SnO_2, Fe_2O_3, ZnO, WO_3, CdS, WS_2, ZnS, and MoS_2 have been used widely for the degradation of organic pollutants; however, they have poor activity without the addition of cocatalyst due to the rapid recombination of electron and hole pair before they migrate to the surface for reaction [6–8]. Metal

fluorides (like zirconium, aluminum, rare-earth metals, and hafnium) have commercial application in isotopic separation and metallurgy and in the preparation of optical and ceramic materials; however, recently, their used has been increased in the field of biosensing, catalysis, as cathode materials for LIBs, super capacitors, and photonics [9–12]. In the past, researchers have used CoF_2 as promising anode material for LIBs. Fu et al. for the first time use CoF_2 as anode material for LIBs [13]. MnF_2 and CaF_2 were used as antimicrobial agents for gram-positive and gram-negative bacteria to find their efficiency [14, 15]. Similarly, Zapała et al. used niflumic acid synthesized with different transition metal complexes for determination of their catalytic and antibacterial activity [16]. Xi et al. used fluorides as disinfectant for the treatment of bacteria [17]. Gajendiran et al. synthesized cobalt ferrite and treat as antimicrobial agent which shows good results against gram-positive bacteria [18]. Arun and Li et al. prepared cobalt and cobalt ferrite NPs and used them as photocatalyst for the degradation of organic dyes like MLB dye and showed efficient results against these dyes as catalyst [19, 20]. Yan et al. used bimetallic fluorides as efficient oxygen reduction catalyst in the defect-enriched carbon nanofibers [21]. Li et al. used cobalt- and fluoride-based photocatalyst for the high-performance evolution of oxygen [22–24]. However, no literature data on CoF_2 is available as catalyst for the degradation of MLB and as antimicrobial agent and used as photocatalyst for the first time with high efficiency by decolorizing and degraded MLB. The novelty of the prepared CoF_2 nanostructures lies in their application, i.e., catalytic and antimicrobial results which were carried out for the first time and not reported in the literature yet.

2. Experimental

2.1. Materials. Cobalt nitrate tetrahydrate, deionized (DI) water, ammonium fluoride, ethanol, etc. were purchased from Sigma-Aldrich and used for the preparation of CoF_2 NPs.

2.2. Synthesis of CoF_2 NPs by Coprecipitation Method. CoF_2 NPs were prepared by dissolving 0.582 g of cobalt nitrate tetrahydrate and 0.182 g of ammonium fluoride in two separate beakers in 4 mL of DI water. The two solutions were then mixed in 30 mL of ethanol in a beaker and stirred for 20 min; immediately, pink color precipitate will appear for CoF_2 NPs; centrifuge and filter the precipitate and dry in an oven for two hours and characterize on various techniques for their structure confirmation and identification. The prepared CoF_2 NPs were then used as catalyst for the degradation of MLB dye as antioxidant and as microbial agent for the treatment of gram-positive and gram-negative bacteria.

2.3. Preparation and Extraction Procedure of MLB Dye for Degradation Studies. Take 3 mg of CoF_2 catalyst powder in three separate I-Chem glass vials and add 10 μL of MLB (10 ppm solution) to each vial; seal the vial, vertex, and shake for 1 minute to promote contact between the sample powder and MLB solution. The substrate will be adsorbed on the surface of catalyst, and after 0 min, 30 min, 60 min, 90 min, and 120 min extracted with 2 mL of isopropyl alcohol (IPA), filter through a 0.45 μm PTFE syringe filter and analyze on a UV/visible spectrophotometer for their degradation studies. The same reaction and extraction procedure was used for the rest of sample preparation and degradation studies. To find the efficiency of synthesized CoF_2 NPs, the amount of catalyst and methylene was kept fixed for all the samples and only varying the time duration.

2.4. Antimicrobial Activity of Cobalt Fluoride NPs. The prepared CoF_2 NPs were examined for their antibacterial activity against *Escherichia coli* (*E. coli*) and *Bacillus subtilis* (*B. subtilis*), by well diffusion and serial dilution method [25, 26] to determine their efficiency against these two bacteria, through a dose-dependent method. In this method, in 1 mL of deionized water, 2 mg of cobalt fluoride was dissolved and sonicate this solution for 30 min. The bacteria under test were purchased from CGMCC (China General Microbial Culture Collection Center). Incubate the bacterial culture containing LB media in a 4 mL tube. Keep the tube at 37°C to achieve the 0.5 standard of McFarland ($1 \times 10^{6-10}$ 8 CFU/mL). Transfer 100 μL of this turbid culture into a Petri dish containing agar media, and disperse bacterial culture in the Petri dish by small beads. Make 4 wells of 6 mm in the Petri dish by metal borer. Add 60 μL to 4 mm well containing different concentrations of 0.25 mg/mL, 0.5 mg/mL, 1.0 mg/mL, and 2.0 mg/mL. Place the Petri dish for 48 h for incubation at 37°C, and calculate the inhibition zone in the unit of millimeter. The antibacterial activity was further confirmed against the experimental bacteria through calculation of minimum inhibition concentration (MIC).

2.5. Minimum Inhibition Concentration (MIC). The minimum concentration at which no visible growth of the tested bacteria occurs is used as indicator to confirm and verify the inhibition of bacteria. CoF_2 NPs and needles of different concentrations (i.e., 7.5, 15, 30, and 60 μg/mL) were added to 4.0 mL LB media broth in four different tubes, and also, 60 μL of culture bacteria to each tube was added. Place these tubes at 37°C for 48 h for incubation and then observe and note the growth of bacteria in each tube.

2.6. Antioxidant Activity. The antioxidant activity (radical scavenging activity) of the prepared CoF_2 NPs and needles was performed as reported in literature [27, 28]. Dissolve different concentrations (0.031, 0.062, 0.125, 0.25, 0.5, and 1.0 mg/mL) of CoF_2 NPs and needles in methanol and add 0.5 mL of 1 mM of DPPH to each tube containing different concentrations and incubate in the dark for 30 min at room temperature. After that, measure the absorbance of both control and sample by UV-Visible Cary 50 at wavelength 517 nm by taking methanol as blank and vitamin C as control blank and calculate their scavenging ability through the following equation.

$$\%\text{Scavenging activity(inhibition)} = \frac{A_c - A^\circ}{A_c} \times 100. \quad (1)$$

A_c is the absorbance of the control.
A° is the absorbance of the tested sample.

3. Results and Discussion

3.1. Physicochemical Characterization. To find the crystal structure and composition of synthesized CoF_2 NPs, XRD techniques were used. The X-ray diffraction studies of the synthesized CoF_2 NPs matched with JCPDS card number 01-072-1179, which shows purity and tetragonal structure for CoF_2 NPs. After drying in oven at 110°C, the crystallinity of the synthesized material improved as evident from the XRD spectrum (Figure 1). The particle size of the prepared cobalt fluoride NPs was calculated by the Scherrer equation which is 36.45 nm after drying.

To find the morphology and shape of the synthesized CoF_2 NPs, SEM was employed. SEM studies of the prepared NPs show flake-type morphology, and the particles agglomerate instead of dispersion as shown in Figure 2. EDX was performed to determine the elemental composition of CoF_2 NPs. EDX studies of NPs are shown in Figure 3, and it exhibits that the synthesized material contains only Co, F, and oxygen with no impurities.

FTIR studies were used to further confirm the prepared CoF_2 NPs. FTIR spectrum of the synthesized material shows its frequency range between 400 cm^{-1} and 4000 cm^{-1}. FTIR spectrum of the prepared material shows that the broad peak of the hydroxyl group for water disappears after drying as shown in Figure 4 which indicate that the material is pure. Other stretching frequencies for CoF_2 NPs appear at 538 cm^{-1}, 1212 cm^{-1}, 1363 cm^{-1}, and 1747 cm^{-1}, which are due to C-H, C-O, and C-F stretching.

UV/visible spectroscopic analysis was performed between 200 and 800 nm to find the wavelength absorption and optical band gap of the synthesized CoF_2 NPs through Kubelka-Munk function. The band gap for CoF_2 NPs was calculated to be 2.79 eV as shown in Figures 5 and 6, before and after drying. Catalytic properties of the prepared CoF_2 NPs depend mainly upon their microstructure, particle size, and surface morphology. XRD studies of the prepared CoF_2 NPs show that after drying the crystallinity of the material improved; also, particles size decreases which increase the surface area, and thus, the catalytic behavior of the CoF_2 NPs increases. Moreover, band gap calculation of the CoF_2 NPs also shows that after drying the crystallite size decreases which decrease the band gap, and thus, their catalytic effect increases as shown in Figure 6 from their band gap calculation through the Kubelka-Munk function.

3.2. Degradation Studies of MLB Dye. Degradation studies of MLB solution (10 ppm) were carried out with the help of UV/visible spectrophotometer (Cary 50) to determine the efficiency of CoF_2 photocatalyst with respect to time and their decolorization rate. Initially, 3.0 mg of CoF_2 catalyst powder is in three separate I-Chem glass vials, and add 10 μL of MLB (10 ppm solution) to each vial, seal the vial,

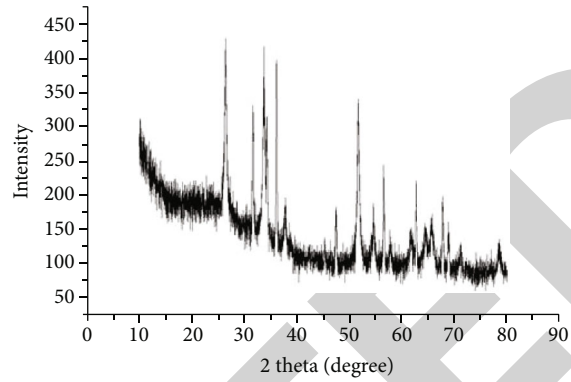

Figure 1: XRD patterns for CoF_2 NPs synthesized by the precipitation method.

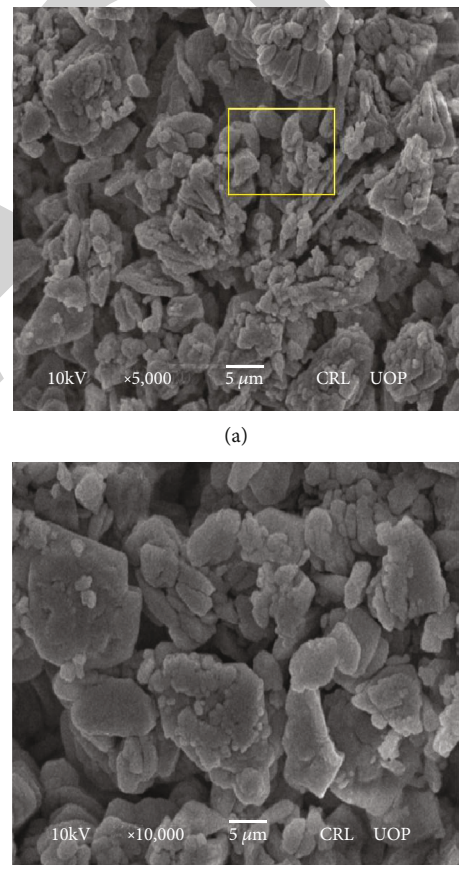

Figure 2: (a, b) SEM micrographs of CoF_2 NPs prepared by simple precipitation method with different magnifications.

vertex, and shake for 1 minute to promote contact between the sample powder and MLB solution. The substrate will be adsorbed on the surface of catalyst, and after 0 min, 30 min, 90 min, and 120 min extracted with 2 mL of isopropyl alcohol (IPA), filter through a 0.45 μm PTFE syringe filter and analyze on a UV/visible spectrophotometer for their degradation studies. The same reaction and extraction procedure was used for the rest of sample preparation and degradation studies. To find the efficiency of synthesized CoF_2

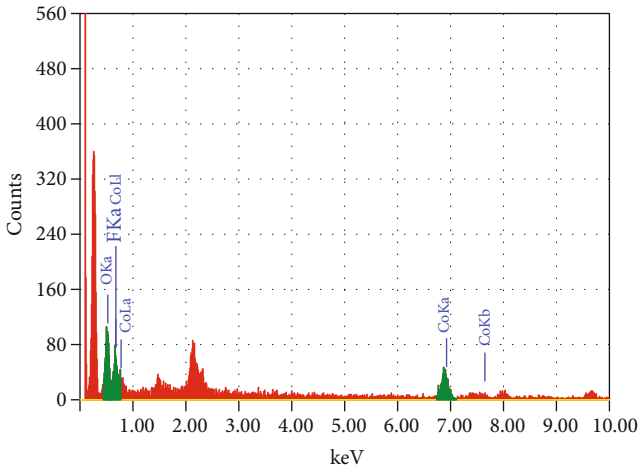

Figure 3: EDX spectrum of the prepared CoF_2 NPs.

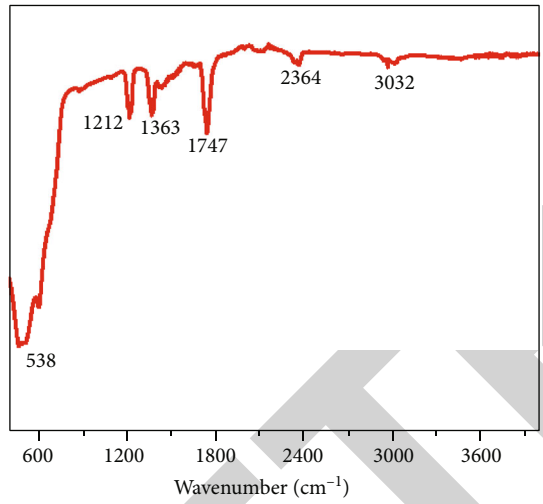

Figure 4: FTIR spectra of prepared CoF_2 NPs.

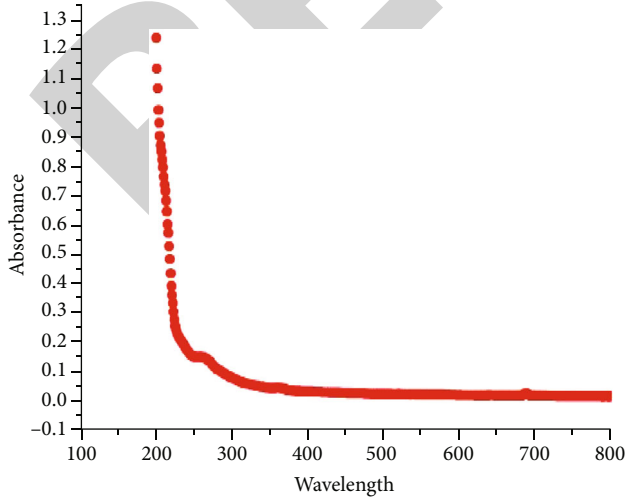

Figure 5: UV-Vis spectra of prepared CoF_2 NPs.

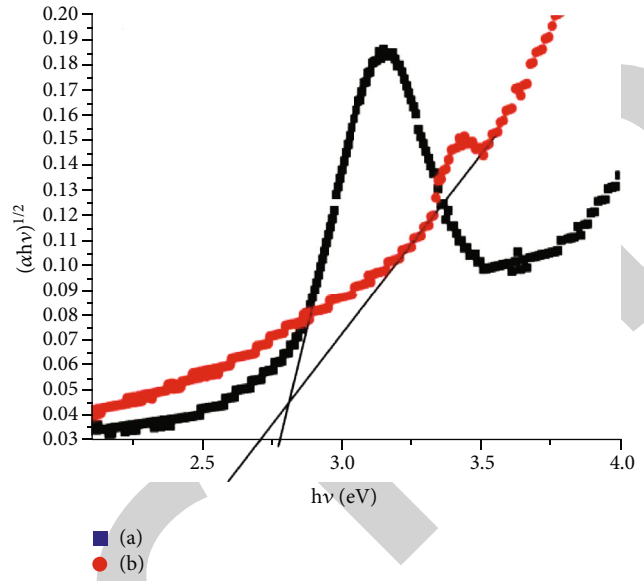

Figure 6: Band gap calculation of CoF_2 NPs (a) before and (b) after drying.

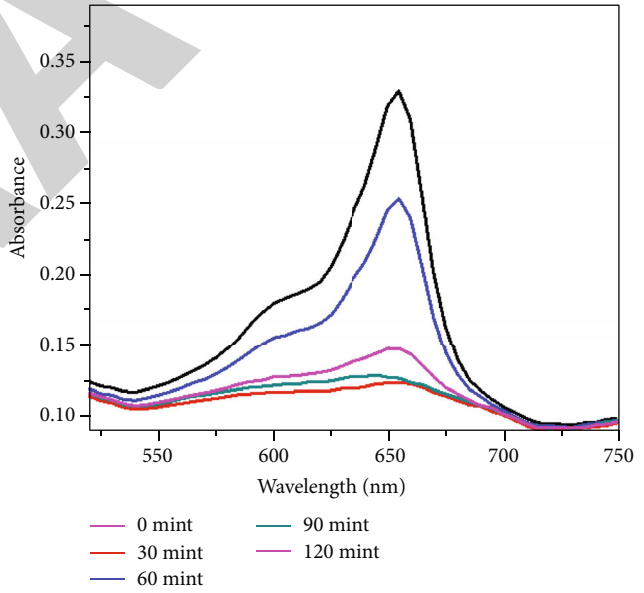

Figure 7: UV/visible spectrum shows the degradation studies of MLB dye.

NPs, the amount of catalyst and methylene was kept fixed for all the samples and only varying the time duration. UV/visible data of the CoF_2 NPs shows that after 0 min no degradation and decolorization occur; after 30 min, 40%; after 60 min, 50% degradation; after 90 min, 70% degradation and decolorization appear in all the samples; and after 120 mint, 90-94% of the samples were degraded with the decrease in concentration with respect to time as indicated from their UV/visible graph (Figure 7).

3.3. Antioxidant Activity. The scavenging activity of CoF_2 NPs is shown in Figure 8. By getting electron or hydrogen

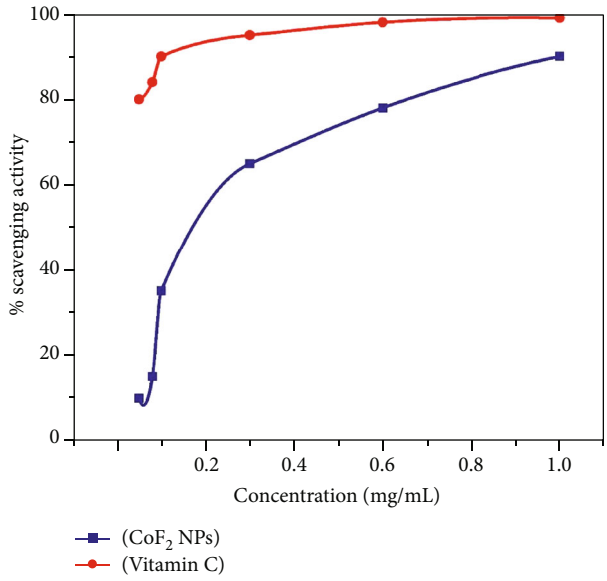

Figure 8: Percentage DPPH scavenging of CoF_2 NPs and vitamin C.

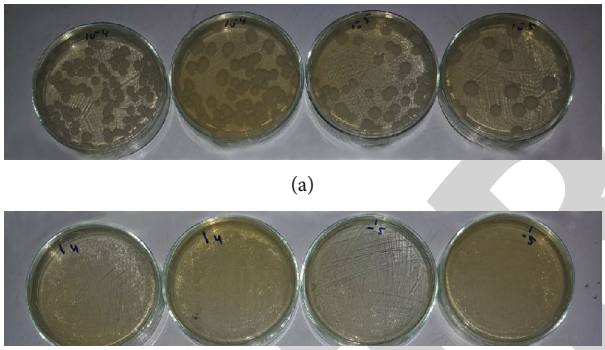

Figure 9: Antibacterial activity of (a) *Bacillus subtilis* and (b) *E. coli* control over CoF_2 NPs.

from the donor atom, 1-diphenyl-2-picrylhydrazyl (DPPH) radical is reduced [29, 30]. It shows high efficiency at concentration of 1 ppm (1 mg/mL). For CoF_2 NPs, the IC_{50} was higher than 1 μg/mL. The mechanisms of antioxidant activity of CoF_2 NPs were unknown; however, it depends upon the transfer of electron from oxygen to nitrogen atom of DPPH and the electronic transition occurs at 517 nm for $n \longrightarrow \pi *$ transition.

3.4. Antibacterial Activity. The antibacterial activity of CoF_2 NPs was tested against gram-positive *B. subtilis* and gram-negative *E. coli* bacteria (Figure 9). The results showed the inhibition of both bacteria at different concentrations of 2, 1, and 0.5 and 0.25, 0.5, 1.0, and 2.0 mg/mL of CoF_2 NPs. These NPs show higher inhibition against *B. subtilis* as compared to *E. coli* at different concentrations. The zone of inhibition (ZOI) for *B. subtilis* was 17 mm at concentration of 1 mg/mL. However, *E. coli* were less susceptible to NPs. The exact mechanism of action of CoF_2 NPs on these bacteria is unknown; however, through oxidative stress, it ruptures the cell membrane by damaging the bacterial lipid layer, DNA, and inhibits bacterial growth. Fluoride act as anticaries, by increasing acidification, reducing bacterial growth, and enhancing permeability of proton through membrane by ATPases [31–33].

4. Conclusion

CoF_2 NPs were prepared through the coprecipitation method and characterized by various techniques, i.e., XRD, SEM/EDX, FTIR, and UV/Vis, to conform their structure. Further catalytic efficiency of CoF_2 NPs was checked against MLB dye for the first time. The UV/visible studies of the synthesized catalyst show that MLB degraded after some time by decolorizing the IPA solution, and also, the concentration of dye decreases with passage of time. Thus, it is concluded that CoF_2 can be used as an efficient catalyst for the degradation of organic dyes (MLB). The prepared CoF_2 NPs show effective antibacterial and antioxidant results against gram-positive and gram-negative bacteria, i.e., *Escherichia coli* (*E. coli*) and *Bacillus subtilis* (*B. subtilis*), for the first time by rupturing their lipid membrane through oxidative stress and acidification.

Data Availability

All the available data are incorporated in the MS.

Conflicts of Interest

The authors declared that they have no conflict of interest.

Acknowledgments

The authors wish to thank Princess Nourah Bint Abdulrahman University Researchers Supporting Project (number PNURSP2022R33), Princess Nourah Bint Abdulrahman University, Riyadh, Saudi Arabia, for financial support.

References

[1] K. E. Drexler, "Engines of Creation: The Coming Era of Nanotechnology," 1986, doubleday978-0-385-19973-5.

[2] K. E. Drexler, *Nanosystems: Molecular Machinery*, Manufacturing, and Computation, New York: John Wiley & Sons, 1992.

[3] A. Hubler, "Digital quantum batteries: energy and information storage in nanovacuum tube arrays," *Complexity*, vol. 15, no. 5, 2010.

[4] N. Ahmad, M. Jabeen, Z. U. Haq et al., "Green fabrication of silver nanoparticles using Euphorbia serpens Kunth aqueous extract, their characterization, and investigation of its in vitro antioxidative, antimicrobial, insecticidal, and cytotoxic activities," *BioMed Research International*, vol. 2022, 11 pages, 2022.

[5] M. Iftikhar, M. Zahoor, S. Naz et al., "Green synthesis of silver nanoparticles using Grewia optiva leaf aqueous extract and isolated compounds as reducing agent and their biological activities," *Journal of Nanomaterials*, vol. 2020, 2020.

[6] D. Lyon and A. Hubler, "Gap size dependence of the dielectric strength in nano vacuum gaps," *IEEE Transactions on*

Dielectrics and Electrical Insulation, vol. 20, no. 4, pp. 1467–1471, 2013.

[7] R. Saini, S. Saini, and S. Sharma, "Nanotechnology: the future medicine," *Journal of Cutaneous and Aesthetic Surgery.*, vol. 3, no. 1, pp. 32-33, 2010.

[8] A. Belkin, A. Hubler, and A. Bezryadin, "Self-assembled wiggling nano-structures and the principle of maximum entropy production," *Scientific Reports*, vol. 5, no. 1, 2015.

[9] J. H. Yang, H. J. Yan, X. L. Wang et al., "Roles of cocatalysts in Pt-PdS/CdS with exceptionally high quantum efficiency for photocatalytic hydrogen production," *Journal of Catalysis*, vol. 290, pp. 151–157, 2012.

[10] M. Wojciechowska, M. Zielinski, and M. Pietrowski, "MgF_2 as a non-conventional catalyst support," *Journal of Fluorine Chemistry*, vol. 120, no. 1, pp. 1–11, 2003.

[11] A. Gul, Fozia, A. Shaheen et al., "Green synthesis, characterization, enzyme inhibition, antimicrobial potential, and cytotoxic activity of plant mediated silver nanoparticle using Ricinus communis leaf and root extracts," *Biomolecules*, vol. 11, 2021.

[12] M. Pietrowski, M. Zielinski, and M. Wojciechowska, "High-selectivity hydrogenation of chloronitrobenzene to chloroaniline over magnesium fluoride-supported bimetallic ruthenium-copper catalysts," *ChemCatChem*, vol. 3, no. 5, pp. 835–838, 2011.

[13] M. Pietrowski, "Selective hydrogenation of ortho-chloronitrobenzene over Ru and Ir catalysts under the conditions of the aqueous-phase reforming of bioethanol," *Green Chemistry*, vol. 13, no. 7, p. 1633, 2011.

[14] M. Zielinski, M. Pietrowski, A. Kiderys, M. Kot, and E. Alwin, "A comparative study of the performance of Pt/MgF_2, Ir/MgF_2 and Ru/MgF_2 catalysts in hydrogenation reactions," *Journal of Fluorine Chemistry*, vol. 195, pp. 18–25, 2017.

[15] A. Kiderys, M. Pietrowski, and I. Tomska-Foralewska, "Synthesis and characterization of new Mg-O-F system and its application as catalytic support," *Catalysis Communications*, vol. 76, pp. 54–57, 2016.

[16] L. Zapała, M. Kosińska-Pezda, Ł. Byczyński et al., "Green synthesis of niflumic acid complexes with some transition metal ions (Mn (II), Fe (III), Co (II), Ni (II), Cu (II) and Zn (II)). Spectroscopic, thermoanalytical and antibacterial studies," *Thermochimica Acta*, vol. 696, p. 178814, 2021.

[17] W. Xi, L. Guo, D. Liu et al., "Upcycle hazard against other hazard: toxic fluorides from plasma fluoropolymer etching turn novel microbial disinfectants," *Journal of Hazardous Materials*, vol. 424, no. Part D, 2022.

[18] J. Gajendiran, S. G. Raj, G. R. Kumar, S. Gnanam, J. R. Ramya, and V. P. Senthil, "Photoluminescence properties and antibacterial activity of $BiFeO_3$ and $BiFeO_3$-$CoFe_2O_4$ composite," *Journal of Electronic Materials*, vol. 51, no. 1, pp. 8–16, 2022.

[19] K. Arun, "A review on plant extract-based route for synthesis of cobalt nanoparticles: photocatalytic, electrochemical sensing and antibacterial applications," *Current Research in Green and Sustainable Chemistry*, vol. 5, 2022.

[20] M. Li, Y. Gu, Y. Chang et al., "Iron doped cobalt fluoride derived from CoFe layered double hydroxide for efficient oxygen evolution reaction," *Chemical Engineering Journal*, vol. 425, p. 130686, 2021.

[21] J. Yan, Y. Huang, Y. Zhang et al., "Facile synthesis of bimetallic fluoride heterojunctions on defect-enriched porous carbon nanofibers for efficient ORR catalysts," *Nano Letters*, vol. 21, no. 6, pp. 2618–2624, 2021.

[22] M. Li, H. Liu, and L. Feng, "Fluoridation-induced high-performance catalysts for the oxygen evolution reaction: a mini review," *Electrochemistry Communications*, vol. 122, p. 106901, 2021.

[23] Z. Jin, H. Li, and J. Li, "Efficient photocatalytic hydrogen evolution over graphdiyne boosted with a cobalt sulfide formed S-scheme heterojunction," *Chinese Journal of Catalysis*, vol. 43, no. 2, pp. 303–315, 2022.

[24] J. Khan, H. Ullah, M. Sajjad et al., "High yield synthesis of transition metal fluorides (CoF_2, NiF_2, and NH_4MnF_3) nanoparticles with excellent electrochemical performance," *Inorganic Chemistry Communications*, vol. 130, p. 108751, 2021.

[25] J. Khan, H. Ullah, M. Sajjad et al., "Controlled synthesis of ammonium manganese tri-fluoride nanoparticles with enhanced electrochemical performance," *Materials Research Express*, vol. 6, no. 7, 2019.

[26] A. EL Moussaoui, M. Bourhia, F. Z. Jawhari et al., "Chemical profiling, antioxidant, and antimicrobial activity against drug-resistant microbes of essential oil from Withania frutescens L," *Applied Sciences.*, vol. 11, no. 11, 2021.

[27] R. Ullah, M. S. Alsaid, A. S. Alqahtani et al., "Anti-inflammatory, antipyretic, analgesic, and antioxidant activities of Haloxylon salicornicum aqueous fraction," *Open Chemistry.*, vol. 17, no. 1, pp. 1034–1042, 2019.

[28] R. Ullah, M. S. Alsaid, A. A. Shahat et al., "Antioxidant and hepatoprotective effects of methanolic extracts of Zilla spinosa and Hammada elegans against carbon tetrachlorideinduced hepatotoxicity in rats," *Open Chemistry.*, vol. 16, no. 1, pp. 133–140, 2018.

[29] J. Khan, H. Ullah, M. Sajjad, A. Ali, and K. H. Thebo, "Synthesis, characterization and electrochemical performance of cobalt fluoride nanoparticles by reverse micro-emulsion method," *Inorganic Chemistry Communications*, vol. 98, pp. 132–140, 2018.

[30] S. Ahmad, N. M. AbdEl-Salam, and R. Ullah, "In vitro antimicrobial bioassays, DPPH radical scavenging activity, and FTIR spectroscopy analysis of Heliotropium bacciferum," *Biomed Research International*, vol. 2016, 12 pages, 2016.

[31] Y. T. Teng, S. S. Pramana, J. F. Ding, T. Wu, and R. Yazami, "Investigation of the conversion mechanism of nanosized CoF_2," *Acta*, vol. 107, pp. 301–312, 2013.

[32] Z. Li, J. Yang, T. Guang, B. Fan, K. Zhu, and X. Wang, "Controlled hydrothermal/solvothermal synthesis of high-performance LiFePO4for Li-ion batteries," *Small method*, vol. 5, no. 6, p. 2100193, 2021.

[33] L. F. Olbrich, A. W. Xiao, and M. Pasta, "Conversion-type fluoride cathodes: current state of the art," *Current Opinion in Electrochemistry*, vol. 30, p. 100779, 2021.